POAC'25
St. John's, Newfoundland and Labrador, Canada

Proceedings of the 28th International Conference on Port and Ocean Engineering under Arctic Conditions
Jul 13-17, 2025
St. John's, Newfoundland and Labrador
Canada

Iceberg-Seabed Interactions - Balancing Sediment Reaction and Environmental Driving Forces

Mark Fuglem[1], Tony King[1], John Barrett[1],
[1] C-CORE, St. John's, Canada

ABSTRACT

Determining the risks of gouging icebergs to subsea equipment and pipelines is challenging, given the infrequency of gouge events and the complexities of the processes involved. Relevant factors include the randomness of iceberg shapes, the environmental driving forces acting on the icebergs, and the sediment resistance forces given the influence of bathymetry and sediment type. Each factor has its modelling challenges and uncertainties. Validation of gouge models against measured furrow and pit frequencies and characteristics is critical, but also challenging. Gouge events off Newfoundland and Labrador are infrequent, vary with location and are costly to survey. In interpreting gouge survey data, the dates of the gouges need to be estimated, and the extents of infill and erosion by bottom currents during the period since the gouge was created assessed.

This paper describes initial modelling efforts carried out to explain observed gouge populations. The longer-term goal is to reduce uncertainties regarding gouge processes and thereby help improve future subsea equipment design. Key processes are reviewed, and different modelling approaches are considered. Furrow data from a good-quality subsea survey is analyzed to provide furrow width and depth distributions for model validation. A set of simplified models is implemented within a stochastic framework to obtain distributions of furrow widths and depths, accounting for variations in sea slope, environmental driving forces, random iceberg shapes, and seabed resistance to scouring for the types of seabed sediments in the region. A sensitivity analysis is performed to assess how different input parameters and model assumptions affect the simulated furrow populations and their alignment with observed data. Gaps in our understanding of gouge processes are identified, and improvements in models and survey methods are recommended.

KEYWORDS: Ice gouge, ice furrow, environmental driving force, sediment reaction force

NOMENCLATURE

The nomenclature for ice gouges in ISO 19906:2019 is followed here. An ice gouge is a disturbance of seabed soils by an ice feature. Gouges are further distinguished between events in which a sea ice ridge or iceberg keel drags along the seabed (evidenced by furrows, i.e. linear incisions) and those in which the keel contacts the seabed but insufficient momentum and driving force are available to form a furrow (evidenced by pits, i.e. areal incisions). Infill is sediment subsequently deposited in an ice gouge through natural processes.

BACKGROUND AND OBJECTIVES

When installing subsea equipment and pipelines in offshore regions with icebergs of significant draft, design for direct ice contact or indirect loads through soil deformation will need to be considered if the annual probability of interaction exceeds accepted limits. For equipment above the seabed, freely floating and gouging icebergs need consideration. For equipment placed in excavated drill centres (EDCs) or placed in trenches and covered, gouging icebergs need consideration. Design loads will be determined based on the limit states considered, the frequency of iceberg interactions, the ice strength in the case of direct contacts, and the forces transmitted through the sediment in the case of indirect interactions.

Observed gouges on the Grand Banks and banks off Labrador tend to be relatively wide and shallow. The sediment types are mostly post-glacial sands and gravels. The gouges are formed by the keels of deep draft icebergs, which are often quite rounded. In comparison, gouges in near-shore regions in the Beaufort Sea are formed by sea ice ridge keels, often in clay soils. Gouges there can be relatively narrow and deep. Much of the early work on modelling gouge processes was carried out with Beaufort conditions in mind. Application of these models to Grand Banks conditions results in an underestimation of scour depths. Questions have arisen as to whether the soil strengths are overestimated or the driving forces are underestimated.

A few key studies related to this topic are mentioned. Woodworth Lynas et al. (1999) provide a very informative overview of gouge processes based on fieldwork in which scours off Labrador were examined using a submersible. They showed that iceberg furrowing can occur over significant distances, and moderate elevation changes occur without major changes in the depth and width of the furrows. They reference an iceberg that flipped over after gouging, in which boulders were embedded in the ice. They found that pieces of ice were still embedded in the furrow sediments shortly after the gouge event and that pockmarks occurred along older furrows, showing where ice pieces were likely embedded and then melted. Striations observed at the bottoms of the furrows look like they were produced by rocks embedded in the ice. Jordaan (2023), based on triaxial tests, shows that ice will lose strength due to pressure softening under high volumetric pressures. Furthermore, ice at the surface of an iceberg could be near the melting temperature, and hence fail more easily. Diemand (1984) shows that the gradient in temperature with penetration into the iceberg can be quite gradual in colder water when melting is slow. Even in summer, the water on the Grand Banks remains relatively cold at depth. These findings indicate that there could be significant ice erosion during furrowing. This would have important implications on the development of furrow models: many present models treat the ice as rigid with a fixed keel attack angle, whereas the attack angle could change (and even the furrow depth) as the ice erodes.

McKenna et al. (1999) and Croasdale et al. (2000) conducted related studies in which a stochastic model for iceberg gouging was implemented. Considerable effort went into modelling the different environmental forces, icebergs of varied sizes and stability, and seabed resistance to scouring. The work here borrows from some of their methods.

This project was initiated to resolve discrepancies between modelled and measured furrow dimensions on the Grand Banks. The steps are as follows.

- Review past work on data collection and modelling related to iceberg gouging on the Grand Banks,
- Select an appropriate set of gouge data for model validation. Emphasis has been placed on furrows where the associated event can be treated as quasi-static, i.e. inertial forces are relatively small and the scour width and depth remain fairly constant or change

gradually.

- Implement a stochastic model for evaluating different model assumptions regarding quasi-static furrowing processes. This includes the selection of an appropriate measure for how well the modelled and observed distributions of furrow widths and depths match.
- Conduct a sensitivity analysis showing the influence of different models and model parameters on the goodness-of-fit.
- Identify key areas of uncertainty and suggest steps for improving data collection and models to reduce this uncertainty and associated required levels of conservatism in designs.

OVERVIEW OF PHYSICAL PROCESSES AND APPROACH

The processes influencing the creation of gouges and the population of observed gouges are discussed below with reference to Figure 1.

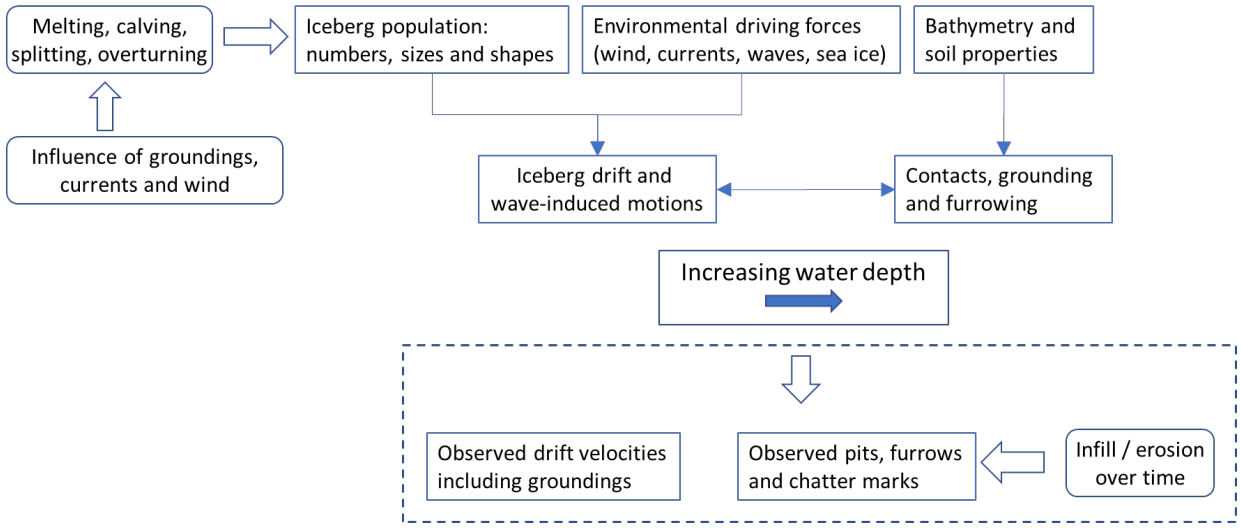

Figure 1. Factors influencing observed gouges, pits and chatter marks

Furrowing and pitting events occur when freely floating icebergs move into a region where the water depth is less than the iceberg draft. On subsequent contact with the seabed, varied interaction dynamics can occur depending on the mass and shape of the iceberg, its initial drift velocity and kinetic energy, the sea slope and soil characteristics, the change in driving forces as the iceberg starts to decelerate, and the ice strength.

If the seabed slope is small in the direction that the iceberg travels, the iceberg may start furrowing, with the furrow depth increasing as the iceberg moves upslope. Alternatively, if the seabed slope in the direction the iceberg travels is steep, the iceberg may plough into the slope following first contact, creating a pit. Icebergs have been observed to ground and stay at the location for hours or days. The keel or iceberg could fracture and calve ice, thereby losing sufficient draft, then either floating away or starting to furrow. If a furrowing iceberg can pitch relatively easily, it may pitch and heave given the driving and sediment resistive forces enough to allow it to furrow a more significant distance up-slope.

The modelling approach is presented in Figure 2. Icebergs having a free-floating draft of 100 m are considered. Other iceberg dimensions are sampled from a joint probability distribution of iceberg draft, length, width and mass. A furrow slope is sampled from a distribution determined from observed furrow data. The iceberg's free-floating drift velocity is sampled

from a distribution of observed drift speeds of larger icebergs. The pitch and heave stiffness are taken from an idealized model of iceberg shape given as a function of waterline length, width and draft. At each time step, as the iceberg moves forward, a solver is used to determine the new furrow depth and width, horizontal and vertical sediment reaction forces and iceberg heave and pitch. Given the horizontal sediment reaction force, the reduced iceberg velocity and kinetic energy are determined at each time step. The furrow width and depth are recorded at 5 m intervals until the iceberg has stopped (i.e. once the seabed resistance force exceeds the driving force and the iceberg momentum is used up). As furrows tend to infill over time, a simple infill rate is applied to reduce the modelled furrow depth, assuming that the furrow occurred at a random point in time in the past. The resulting joint distribution of furrow width and depth is then compared to the observed distribution, and the effects of different model inputs and assumptions on the goodness-of-fit are evaluated.

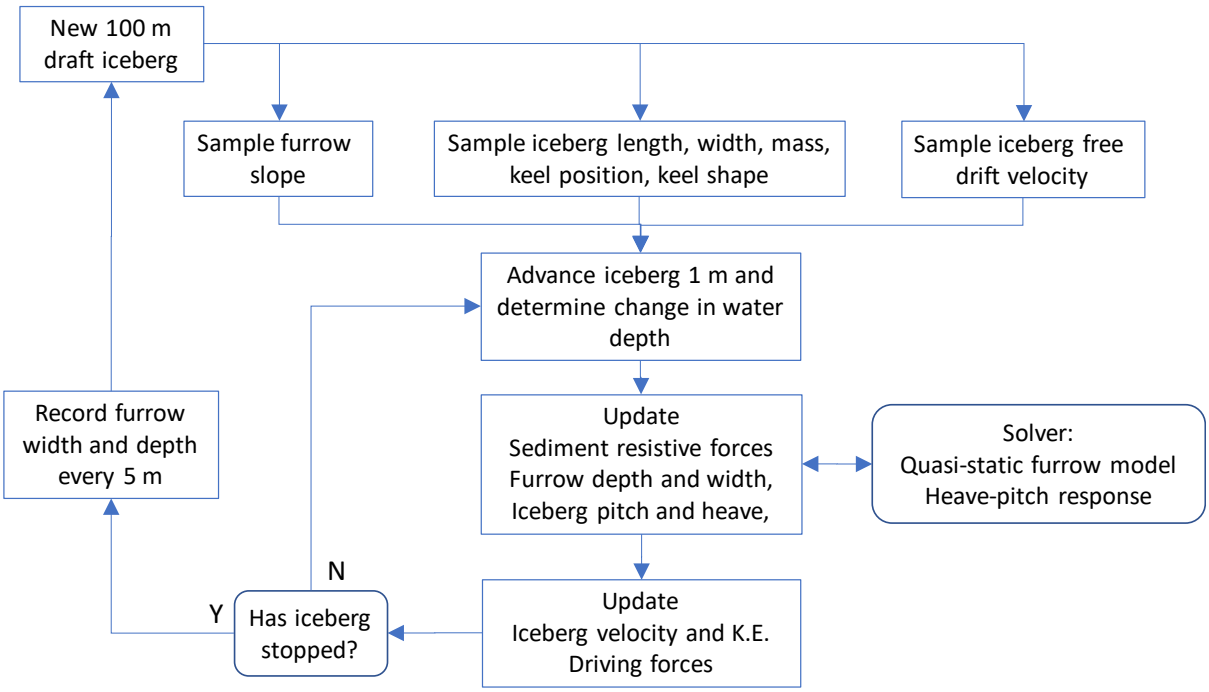

Figure 2. Modelling approach

OBSERVED GOUGE DATA

Substantial effort has been made to measure gouges on the Grand Banks to better define gouging rates, gouge dimensions and the extent of sub-gouge deformations. Over time, significant improvements in measurement accuracy have been achieved. For model validation, consistent and accurate data is needed. Data from the 2004 Grand Banks survey (see Sonnichsen and King, 2011) is utilized. This data consists of measurements with excellent resolution and includes gouge parameters for individual profiles (measurements from cross-section profiles along furrows and pits) as well as summary statistics for whole furrows and pits. There is also a qualitative assessment of the amount of infill for each gouge.

Profiles from the 2004 survey for furrows in water depths less than 100 m were extracted, and the furrow width and maximum depth were determined, typically at 5 m spacings (see Figure 3 for definitions). The mean profile width was 31.8 m, and the mean maximum depth was 0.23

m. Figure 4 shows the histograms of water depth, profile width and profile maximum depth. Figure 5 shows the relationship between width and maximum depth and exceedance plots for depth and width.

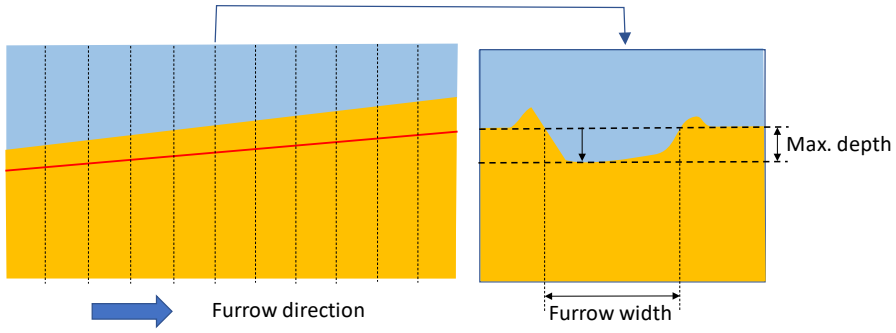

Figure 3. Furrow parameters determined at each profile at 5 m spacing

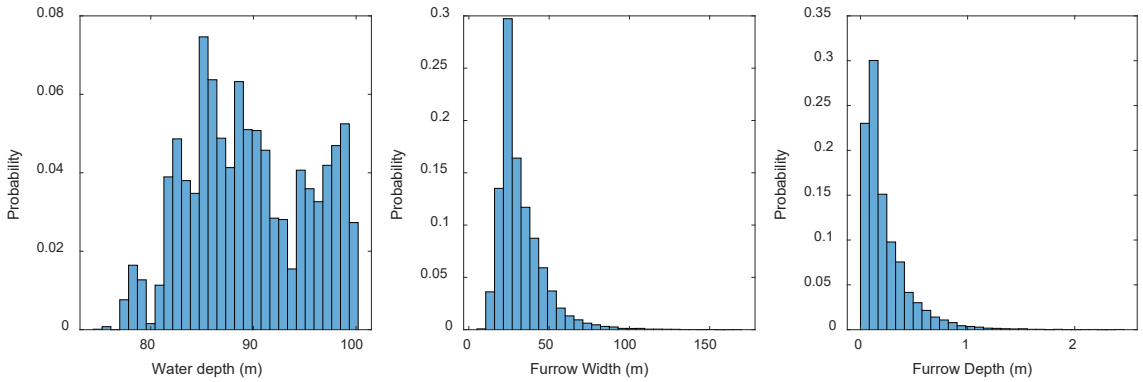

Figure 4. Histogram of furrow width and depth (2004 scour survey)

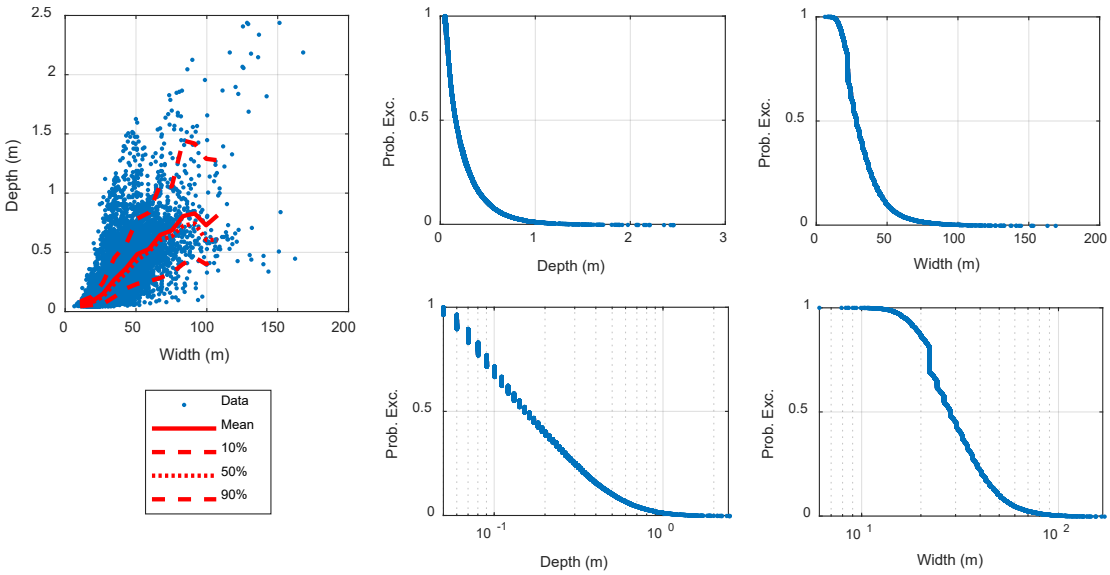

Figure 5. Scatter diagram and exceedance probability plots for furrow width and depth

Figure 5 is used as the basis for assessing the quasi-static furrow model. There is a fairly strong correlation between profile width and maximum depth. It should be cautioned that some of the

higher depth and width combinations may be associated with inertial effects where the iceberg keel comes in contact with a rise or drop. These occurrences are relatively infrequent. Another observation is that over 80% of the profiles have a width greater than 20 m. This has not yet been explained fully, but could relate to the five cm lower limit that was applied in the 2004 survey on the maximum depths recorded. Another possibility is that narrower keels tend to shear off or erode.

Furrows observed on the seabed are infilled to some degree, so the measured depths will underestimate the original depths. The degree of infill for the total furrow population will be a function of factors such as sediment type, bottom currents, water depth and the wave regime. Furrows measured in some sediment types and locations can be extremely old, whereas in other situations they can infill in the order of a few years. Unfortunately, furrows are very difficult to date. Repetitive mapping surveys are very useful, but it takes a long time to accumulate sufficient data given the low frequency of gouge events.

Relatively few new furrows were identified and measured in the 2004 survey. Based on a sample of five furrows considered new, the average furrow depth was 0.4 m. This compares to an average furrow depth of 0.2 m, which implies an average infill rate of 50 percent. This is also the rate one expects for a uniform furrow occurrence rate and uniform infill rate, having lasted over a long period. In the stochastic furrow model, the modelled furrow depth is reduced by 0% to 100% based on a uniform random distribution.

ENVIRONMENTAL DRIVING FORCES AND ICEBERG RESPONSE

The equation of motion for a furrowing iceberg is as follows:

$$M\ddot{x} + D\dot{x} + Kx = F_{Furrow} + F_{wind} + F_{current} + F_{wave} + F_{ice} \quad (1)$$

The parameters x, $\dot{x}$ and $\ddot{x}$ are six-element arrays for the position, velocity and acceleration of the iceberg at and through its center of gravity (CG) in the x, y and z directions and pitch, roll and yaw. M is the inertia matrix for the iceberg, including hydrodynamic added mass effects. D represents drag and damping effects given the iceberg velocity in six degrees of freedom. K represents the hydrostatic stiffness response of the iceberg to heave, pitch and roll. Given the random shapes of icebergs, this will be non-linear for larger responses with coupling between the heave, pitch and roll. With large enough rotation, the iceberg may move to a new stability point, for which the iceberg draft and hydrostatic coefficients change. F_{wind}, $F_{current}$, F_{wave} and F_{ice} represent driving forces acting on the iceberg due to wind, current, waves and sea ice. F_{Furrow} represents the seabed reaction force acting on the iceberg at the location where its keel interacts with the seabed.

For quasi-static solutions, the inertial terms do not apply. The non-inertial force terms are described below, with reference to Figure 6. In cases where the iceberg is no longer decelerating, the gouge forces should approximately balance the driving forces as long as there is no abrupt change in bathymetry, sediment type or environmental forces.

As an iceberg moves toward the slope and starts to contact, the sediment will resist the keel's movement, resulting in a resistive force with horizontal and vertical components. If the net driving force is not through the vertical line intersecting the keel contact position, the iceberg will start to yaw, such that the keel ends up behind the centre of mass.

The vertical reaction force at the keel will cause the iceberg to heave upwards. The horizontal

and vertical forces at the keel will both act to pitch the iceberg. The pitch moment arm associated with the horizontal force is the vertical distance between the iceberg's centre of mass and the seabed. The pitch moment arm associated with the vertical force equals the horizontal distance between the seabed contact point and the centre of mass.

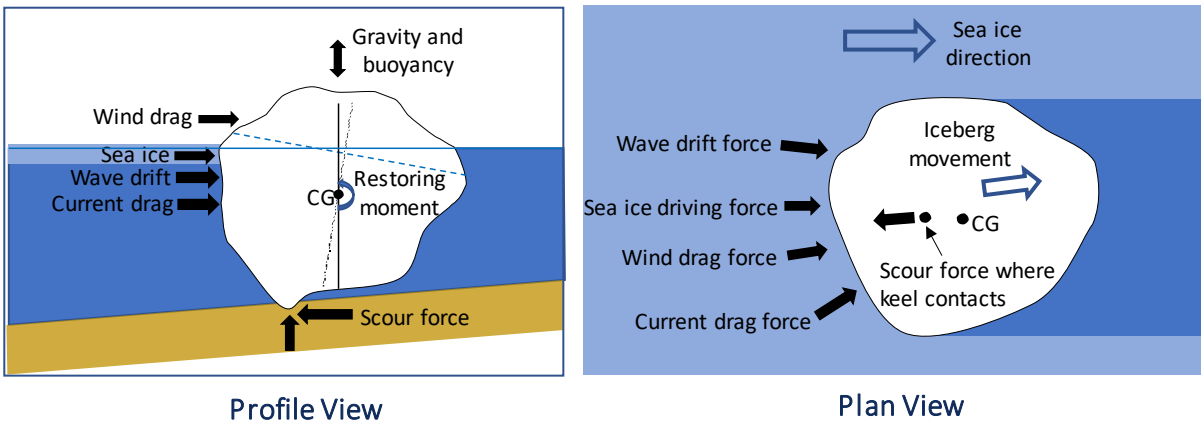

Figure 6. Forces acting on a gouging iceberg

The length of the resulting furrow will depend on the slope, the iceberg's initial momentum, the driving forces on the iceberg, and the sediment reaction forces. The sediment reaction forces will depend on the keel shape and on how easily the keel lifts, given the heave and pitch stiffness of the iceberg.

Following McKenna et al. (1999), a generalized iceberg shape is considered. Icebergs of different dimensions (length, width and draft) are sampled from an appropriate joint probability distribution for the region, and the generalized shape is transformed to match these dimensions. Based on this shape, the iceberg's heave and pitch stiffness response to any applied vertical and horizontal force can be determined. In the next phase of work, detailed actual profiles of large icebergs, as measured over the past decade, will be considered.

A freely drifting iceberg moving at constant velocity has the wind, current and wave drift forces in equilibrium. The wind drag force is determined using a simple drag equation based on the projected above-water area of the iceberg and the wind speed at a given reference height. The wave-drift force depends on wave height and the relative size of the iceberg to the wavelength. Currents typically vary in magnitude and direction with depth. One approximate estimate (used here) of water drag is to consider the average current over the draft of the iceberg and use a simple drag equation based on the projected underwater area of the iceberg. An alternative solution is to determine the drag at different depths, given the current and projected iceberg width at each depth, then sum these.

Once the iceberg starts to decelerate due to seabed reaction forces, the driving forces will no longer be in equilibrium. The water drag force will increase as the relative velocity between the current and the iceberg increases. The wind speed is generally much higher than the iceberg's speed, so wind drag will remain approximately constant as the iceberg decelerates. Wave-drift forces are also relatively independent of the iceberg velocity.

This paper uses the following simplified approach to estimate iceberg driving forces. Based on observations of iceberg trajectories, the free drift velocities are sampled from a gamma distribution with a mean of 0.34 m/s and a standard deviation of 0.23 m/s. For the present work, a simplified model is used in which the iceberg's free drift velocity is assumed to result from a

uniform current with the same velocity (i.e., the combined effects of the variable currents, wind and waves are replaced with an equivalent uniform current). The force, F, which acts on the iceberg as it subsequently starts to decelerate, is determined from the standard quadratic drag equation

$$F = \frac{1}{2}\rho C_D A(u - u_i)|u - u_i| \quad (2)$$

where ρ is the density of seawater, A is the underwater cross-sectional area of the iceberg perpendicular to the relative direction of motion of the current, u is the current speed and u_i is the iceberg speed.

Drag coefficients for uniform currents depend on the shape and roughness of the body and the relative velocity. For large bodies such as icebergs, the Reynolds number is high. Drag coefficients vary significantly with the shape of the body. These include ranges of 0.2 to 0.5 for a rough sphere, 1 to 1.2 for a round cylinder and 2 to 2.2 for a square cylinder with its face normal to the direction of flow. The shapes of icebergs are very complex, so drag coefficients could change significantly and depend on the yaw orientation of the iceberg. The proximity of the seabed can also influence the drag force. Talimi (2025) references unpublished CFD work that showed a significant increase (potentially 40%) in the drag force due to the bottom effect. The analysis showed that in the deep-water case, the iceberg influenced the current flow to a significant depth under the iceberg. Further CFD work, considering different current profiles and iceberg shapes, is warranted.

The above simplified approach approximates the driving force. As a sensitivity check, the driving force is doubled to determine the influence on the modelled furrow profile statistics. In the next phase of work, we will investigate the driving forces in greater detail as well as potential inertial effects. The influence of the iceberg shape on the inertial added mass effect is also important. For example, the added masses for a sphere compared to a cylinder are 1.5 and 2, respectively. There will be a significant bottom effect for added mass.

The keel shape will significantly influence the iceberg furrow depth and width. It is challenging to directly measure a keel's dimensions as it is under the iceberg. Sonar profiles are taken from the side of the iceberg and do not provide accurate information for the keel, given the increased range and the higher angles of the ice face relative to the sonar. An analysis of the keels of measured iceberg 3D profiles resulted in an estimated average keel width of 30.2 m at 0.3 penetration. As an alternative solution, profiles from the lower sides of icebergs were profiled (C-CORE, 2019; Bruce et al., 2021), and a representative (hyperbolic-elliptic) keel shape was determined, assuming that keels would have the same shape as points anywhere on the lower side of an iceberg. The representative keel shape, determined to a depth of 2 m, is shown in Figure 7. The aspect ratio is three to one. For such a keel, and assuming no ice failure, the furrow dimensions will change significantly depending on the orientation of the keel. Note that at 1 m depth, and considering all possible approach angles, the minimum and maximum widths are 7 and 21 m, respectively. At 0.3 m penetration depth, the width for the larger axis in Figure 7 is 11.5 m compared to 30.2 m for the earlier approach. For this work, the keel from Figure 7 is used, with the width doubled and the aspect ratio reduced to two-to-one based on judgment. Sensitivity analyses were carried out with additional increases in width to determine the effect on furrow parameters. In the next phase, additional analysis of keel shapes, including consideration of variance, will be carried out.

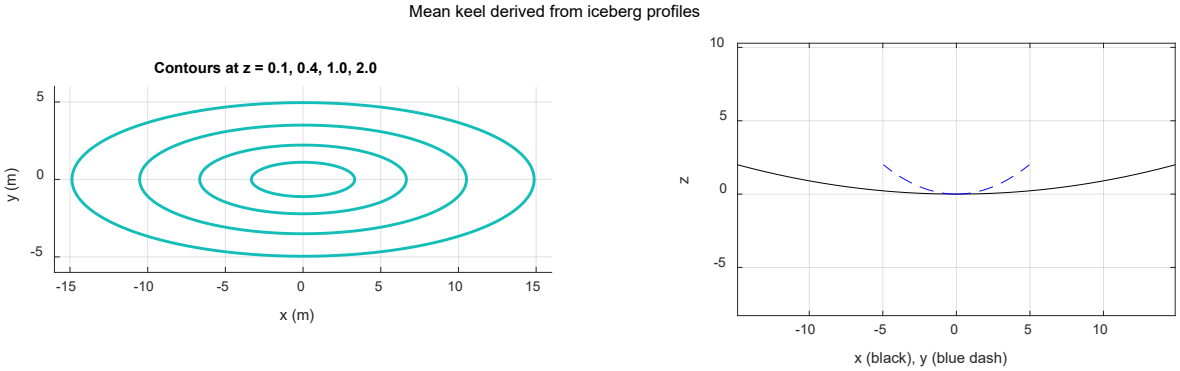

Figure 7. Determined representative iceberg keel shape

SEABED REACTION FORCE

The vertical and horizontal seabed reaction forces F_F^z and F_F^x are required for Equation (1). The seabed reaction force will depend on the shape of the iceberg keel relative to the direction of travel, the furrow depth, the soil properties as a function of depth into the seabed, and potentially the velocity of gouging.

The Pipeline Ice Risk Assessment and Mitigation (PIRAM) project developed a set of engineering models to update industry best practices for risk mitigation and protection of pipeline infrastructure from ice keel loading. PIRAM was primarily focused on high arctic regions, such as the Beaufort Sea, with an emphasis on pressure ridges. Phillips et al. (2012a,b) provide an overview of the PIRAM research program. As part of that program, a series of centrifuge tests were done reflecting furrowing parameters of the Beaufort Sea, which are somewhat narrow and deep compared to those observed offshore Newfoundland on the Grand Banks.

The PIRAM centrifuge test series explored rate and geometric effects in medium to dense sands having relative densities ranging from 40 to 70%. Model ice keels were fabricated with rectangular profiles with keel angles of 15 and 30 degrees. These keel shapes were adopted from earlier work under the PRISE JIP study (Phillips et al., 2005).

C-CORE (2009) proposed a preliminary analytic model for drained frictional soils (see Eqn. (3) and Figure 8) based on the PIRAM data. The horizontal seabed reaction force F_F^x is determined as a function of the furrow width W_F, furrow depth D_S, keel angle, α, and the soil's submerged specific weight, γ' as:

$$\frac{F_F^x}{\gamma' W_F \left(D_F + \frac{W_F}{5}\right)^2} = \begin{cases} \left(\frac{7}{\sin\,\alpha} - 5\right)\left(\frac{(15 - W_F/D_F)}{15}\right) + 5, & W_F/D_F < 15 \\ 5, & W_F/D_F \geq 15 \end{cases} \quad (3)$$

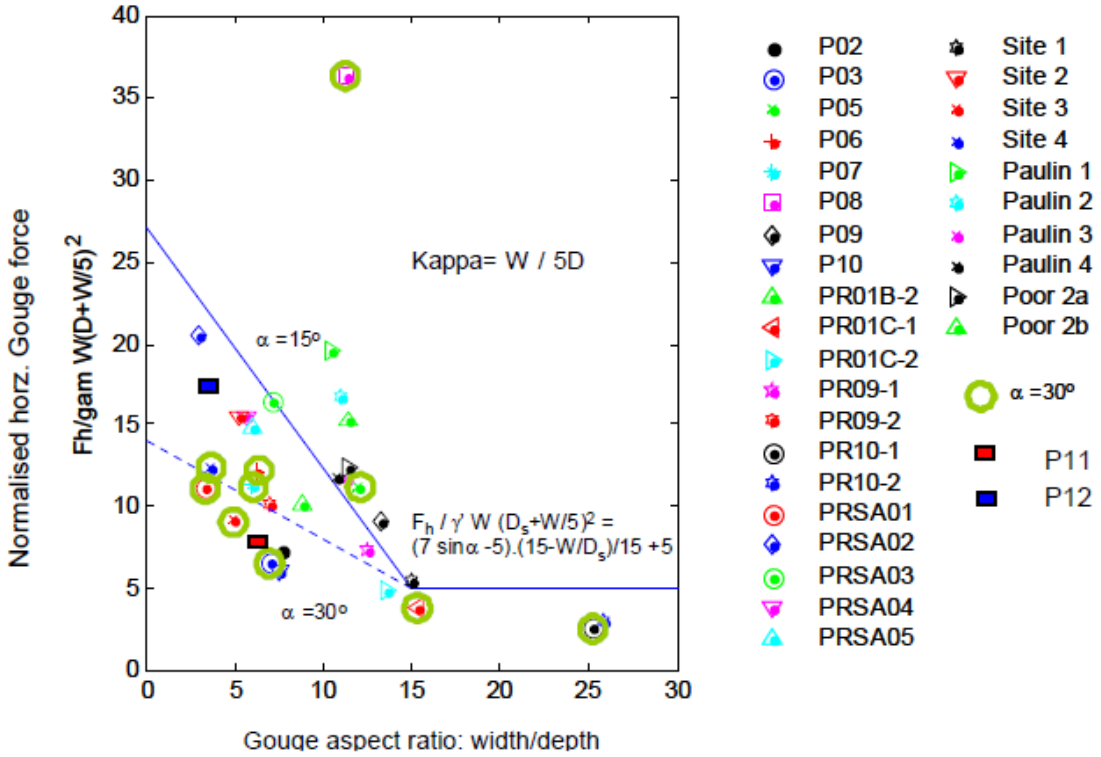

Figure 8. Analytic seabed reaction force model from PIRAM (C-CORE, 2009)

C-CORE (2009) includes a suggestion that the vertical gouge force (F_{scour}^{z}) be set to 0.9 times the horizontal force. Note that the soil is characterized by a single parameter, the soil's submerged specific weight, γ', while the iceberg keel is described in terms of three parameters, W_F, D_S, and α. For width-to-depth ratios less than 15, the force depends on the keel angle, while for values greater than 15, the force is independent of keel angle. One issue with the model was that for wide, shallow furrows, there was only a single centrifuge result on which to base the model. Eqn. (3) thus includes a significant degree of conservatism for such furrows.

Numerical modelling was carried out to provide better estimates of forces for large furrow aspect ratios. The PIRAM data set used for calibration of the numerical analysis is presented in Table 1.

Table 1. PIRAM test parameters and results used for numerical model calibration (converted to full-scale values)

Test	Relative Density (%)	Angle (Deg.)	Depth (m)	Width (m)	W/D (-)	Fh Max (MN)	Fv Max (MN)	Fv/Fh Max (-)	Fh Avg. (MN)	Fv Avg. (MN)	Fv/Fh Avg. (-)
P03	50	30	1.43	10.0	7.00	12.2	10.9	0.89	11.1	10.0	0.89
P06	50	30	2.30	14.4	6.25	47.0	65.2	1.38	37.1	52.9	1.43
P07	40	30	2.40	14.4	5.96	45.4	52.5	1.16	38.6	48.2	1.25
P09	40	15	1.20	16.0	13.3	28.2	32.4	1.15	25.8	29.1	1.13

As described in Barrett et al. (2023), the Coupled Eulerian-Lagrangian (CEL) technique was used to simulate the ice furrowing process using finite element analysis software Abaqus\Explicit. Drained, Mohr-Coulomb, soil parameters were used to represent the sand in calibration to PIRAM data. Capturing dilation behaviour in dense sand is critical in estimating

soil resistance. According to Bolton (1986), the maximum and critical effective friction angle, φ'_{max} and φ'_{crit}, can be correlated to the relative dilatancy index, I_R, as shown in Equation (4), assuming a triaxial strain condition. Using this approach to capture dilation, good correspondence is shown between the test data and numerical analysis, as shown in Figure 9, considering φ'_{crit} to be 33 degrees.

$$\varphi'_{max} - \varphi'_{crit} = \psi = 3I_R \tag{4}$$

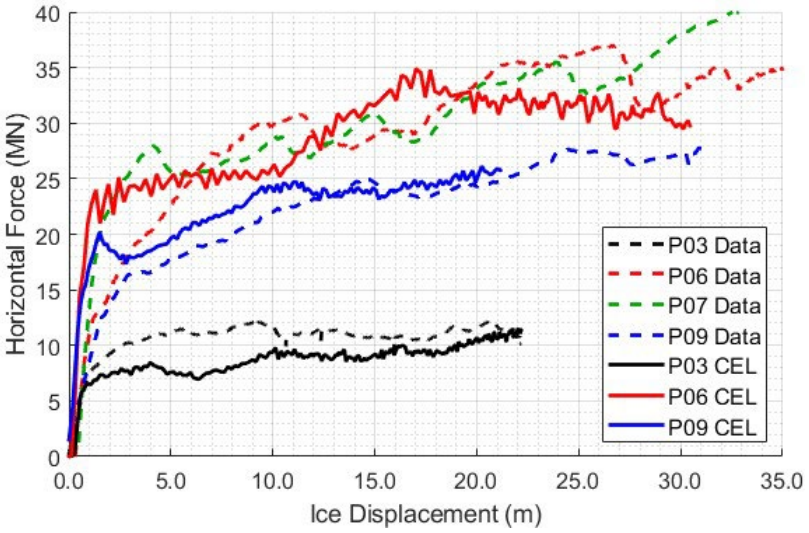

Figure 9. Numerical model calibration to PIRAM data

Iceberg keel shapes were based on the elliptical paraboloid model described previously, with average keel angles between 10 and 15 degrees. For the numerical analysis of wide and shallow furrows, the relative density and critical friction angle used were increased to 75% and 36 degrees, respectively, after a review of cone penetration test data and Pike et al. (2018) with specific reference to the Grand Banks. A high coefficient of friction was also used with the assumption that the sand and gravel particles adhere to the ice surface, creating a roughened surface. The magnitudes of the horizontal forces generated are shown in Figure 10. The vertical-to-horizontal force ratios were found to be 1.4 for 45 m wide ice keels and 1.2 for 12.5 and 25 m wide keels.

A best-fit inverse relationship to all data points is assumed between the normalized horizontal force and W/D (Figure 11). It was found that the dilation of soil in the 12.5 m wide and 0.5 m deep case effectively increases the bearing width of the ice keel to 16 m, and as such, the horizontal force is normalized by an effective width of 16 m, and W/D increases to 32. As the model is applied to explain gouges with large W/D ratios, the fit for smaller W/D ratios is not critical.

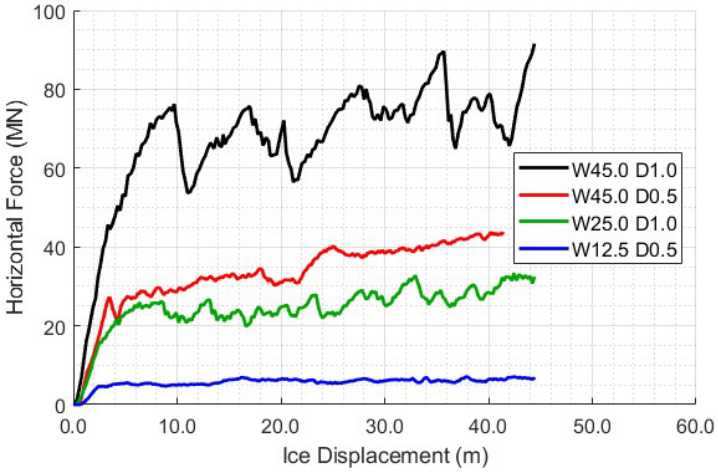

Figure 10. Horizontal ice forces for large W/D ratios

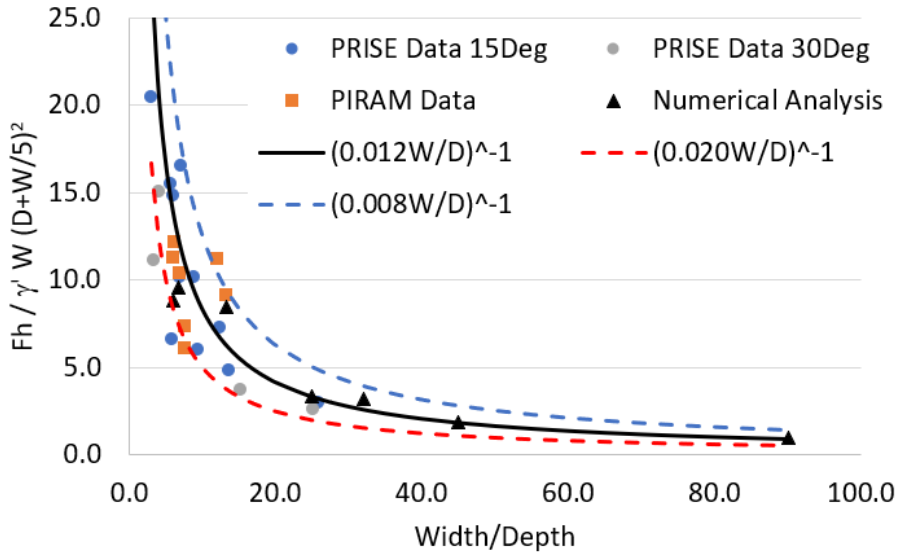

Figure 11. Improved seabed reaction force model

SENSITIVITY ANALYSIS

A sensitivity analysis was conducted to determine the influence of different parameters and model assumptions on how well the observed furrow profile width and depth joint distribution could be replicated. The cases carried out are discussed with reference to Figure 12. The base case assumptions are shown in the column labelled 'Base Case' and the sensitivity case assumptions are shown in the column labelled 'Sens. Case'. Figure 13 shows the results of the Base Case simulation. The simulated furrow depths and widths are too small compared to the measured values. As noted, there appear to be few observed widths less than 25 m. Part of the issue may relate to the inclusion of simulated profiles for the period when the furrows are just starting.

A goodness-of-fit parameter was developed as follows. The observed scatter diagram was divided into areas with equal numbers of occurrences. The mean absolute difference (MAD) in the number of observed and simulated points for these regions was used as the goodness of

fit parameter. The sensitivity cases and influences on fits were as follows.

1. Doubling the driving force results in a moderate improvement in the fit
2. Doubling the widths of the keels had the most significant effect
3. Doubling the widths again makes the fit worse
4. Reducing the ratio of vertical to horizontal seabed resistance force by a significant amount has very little influence
5. Changing the coefficient for the seabed resistance model surprisingly had very little influence
6. Discounting infill makes the model worse, as expected
7. Increasing the added mass effect makes a small improvement

Figure 14 shows the results of the simulation in which the keel width was doubled (which resulted in the largest improvement). It is seen that the furrow depths are still too small.

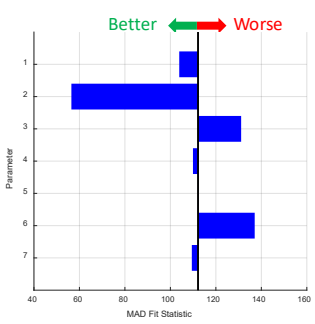

Input Parameter Values	Base Case	Sens. Case
Multiplier on driving force	1	2
Multiplier on keel width	2	4
Multiplier on keel width	2	8
Ratio vert. / horiz. force	1.2	0.8
Seabed reaction force coeff.	0.012	0.008
Infill model	Rand	None
Added mass coeff.	1.5	2

Figure 12. Tornado plot summarizing the results of the sensitivity study

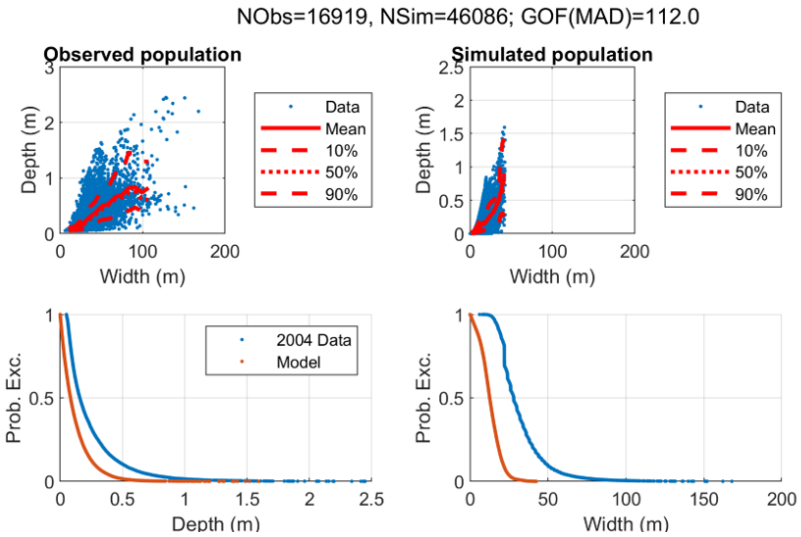

Figure 13. Results of Base Case simulation

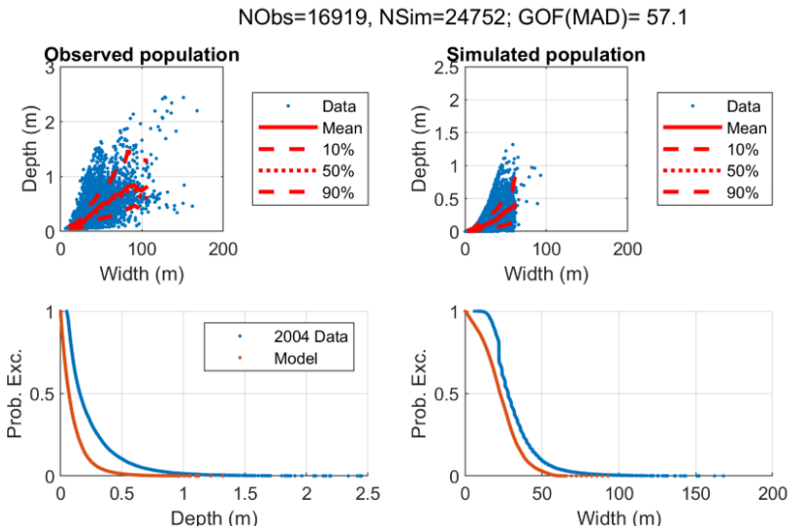

Figure 14. Results of the simulation in which the keel width was doubled

CONCLUSIONS AND RECOMMENDATIONS

A simplified model has been set up for validating assumptions regarding environmental driving forces, sediment resistance and infill rates against observed gouge data. The work to date is preliminary and will be continued. Several comments and conclusions follow.

- At this point, the most important step to improve the model is an increase in the keel widths. Increasing the driving force may help as well. Once the keel widths are improved, the effect of changes in other parameters may change, so the sensitivity analysis should be rerun.
- A key issue to resolve is why the observed profiles include so few narrow furrows. One check will be to remove furrows with a depth of less than five cm from the simulated data, as well as short furrows that would better be classified as pits, and recheck the goodness-of-fit.
- The reason for the small effect of soil strength should be determined.
- There has been a significant number of icebergs profiled over the last 15 years. In the next phase, these will be used to improve the modelling of 1) combined pitch and heave stiffness for rise-up and horizontal and vertical gouge forces and 2) the joint distribution of iceberg mass, length, width, draft and projected areas. CFD modelling can be used to improve estimates of drag and added mass.
- In the next phase, consideration will be given to the change in soil strength with depth and the potential effect of failure of the iceberg keels.

REFERENCES

Barrett, J., Chen, J., Cook, N., Philips, R., and Pike, K. (2023). "SIIBED: Numerical Modeling of Subsea Pipelines and Cables in Ice Prone Region." OTC-32243-MS. Offshore Technology Conference, May 1-4, Houston, Texas.

Bolton, M., 1986, The strength and dilatancy of sands, Geotechnique 36, No. 1, 65-78

Bruce, J., Yulmetov, R., King, T., Ralph, F., and Younan, A., 2021. Development of iceberg profiling technology (OMAE2021-62950). In: Proceedings of the ASME 2021 40th International Conference on Ocean, Offshore and Arctic Engineering (OMAE21). June 21-30, Online.

C-CORE, 2009, Pipeline Ice Risk Assessment and Mitigation (PIRAM) – Draft Final Report, C-CORE Report R-09-019-490v2.0, December 2009

C-CORE. 2019. "Iceberg Keel Geometry." Report No. R-19-021-1478, Prepared for Petroleum Research Newfoundland and Labrador, Revision 4.0, November.

Croasdale & Associates Ltd., 2000, Study of iceberg scour & risk in the Grand Banks region, PERD/CHC Report, no. 31-26 (March 2000).

Diemand, D., 1984, Iceberg Temperatures in the North Atlantic -Theoretical and Measured, CRST

Jordaan, I., 2023, Mechanics of Ice Failure – An Engineering Analysis, Cambridge University Press

ISO 19906:2019 Petroleum and natural gas industries — Arctic offshore structures

McKenna, R., Crocker, G. and Paulin, M., 1999, Modelling Iceberg Scour Processes on the Northeast Grand Banks

Phillips, R. and Barrett, J. 2012a, PIRAM: Pipeline Response to Ice Gouging, OTC Arctic Technology Conference, Houston, Texas, USA, December 2012.

Phillips, R., Clark, J. I. and Kenny, S., 2005, PRISE: studies on gouge forces and subgouge deformations. 18th Int Conf Port & Ocean Engineering under Arctic Conditions, Vol. 1, p75-84.

Phillips, R., King, T. and Bruce J., 2012b, PIRAM: Pipeline Ice Risk Assessment and Mitigation overview, Proceedings of the 2012 9th International Pipeline Conference (IPC2012), September 24-28, Calgary, Alberta, Canada.

Pike, K. and Blundon, A. (2018a). Simulating the Response of Untrenched Flowlines due to Iceberg-Flowline-Soil Interaction. Proceedings of the ASME 2018 37th International Conference on Ocean, Offshore and Arctic Engineering. OMAE2018-78128.

Sonnichsen, G. and King, T., 2011, 2004 Grand Banks Iceberg Scour Survey, POAC

Talimi, V., 2025, Personnal Communication.

Woodworth-Lynas, C., Josenhans, H., Barrie, J., Lewis, C., and Parrott, D., 1991, The physical processes of seabed disturbance during iceberg grounding and scouring, Continental Shelf Research